

A Study of Imprint-Specific Defects in the Step and Flash Imprint Lithography Process

J. Perez, K. Selinidis, S. Johnson, B. Fletcher, F. Xu, J. Maltabes,
I. McMackin, D. Resnick, S.V. Sreenivasan^{†‡}

Molecular Imprints, Inc., 1807C West Braker Lane, Austin TX 78758, USA

ABSTRACT

Researchers have demonstrated that imprint lithography techniques have remarkable replication resolution and can pattern sub-5nm structures. However, a fully capable lithography approach needs to address several challenges in order to be useful in manufacturing. For successful manufacturing insertion of Step and Flash Imprint Lithography (S-FILTM) into a broad set of applications such as photonics, magnetic storage, and integrated circuits (ICs), the following practical process related challenges need to be addressed: (i) Printing sub-50nm structures with non-uniform pattern densities; (ii) Precise alignment and overlay with the ability to mix-and-match with photolithography; (iii) Availability of 1X templates; (iv) Achieving appropriate throughput for acceptable cost of ownership; and (v) Minimizing template and imprint process-induced defects to allow acceptable process yields. The last challenge – the ability to achieve low defect densities – is desirable for all applications. However, it is one of the biggest challenges for S-FIL to be accepted in IC fabrication. This article specifically focuses on this last challenge and presents the current status of defect reduction in S-FIL technology.

The article starts out by providing a brief background of S-FIL technology, and by including a discussion of the overall status of S-FIL technology in Section 1. Next, an overview of the experiments performed including the defect inspection approaches used is provided in Section 2. Section 3 introduces the classes of defects that are relevant to the S-FIL process. It also provides recent defect data for each of these classes. Section 4 presents defect data gathered over the last three years and provides defect reduction trends over this period. Section 5 discusses the topic of template lifetime. Finally Section 6 provides some concluding remarks. The defect data presented here is based on a large number of short-loop experiments based on optical inspection of templates and wafers; these data are complemented by a modest number of high resolution e-beam inspections to provide insight into S-FIL specific defects at leading edge line widths.

Keywords: S-FIL specific defects, template defect reduction, wafer defect reduction

1 INTRODUCTION

Nanoimprint lithography is considered a cost-effective alternative to photolithography for emerging nano-resolution applications including photonic crystals for high-brightness LEDs, patterned magnetic media for next generation hard disk drives, sub-wavelength optical components, and biochemical analysis devices. Imprint lithography is also on the ITRS roadmap for CMOS memory and logic devices at the 32nm node and beyond¹. Researchers have demonstrated that nanoimprint lithography techniques have remarkable replication resolution and can pattern sub-5nm structures². For imprint lithography to be viable in manufacturing, it should not only allow sub-50 nm patterning capability, it should substantially retain the overall benefits of photolithography in other areas such as overlay, defectivity, and cost of ownership. Nanoimprint lithography techniques are essentially molding techniques where patterns etched into a template (master mold) are replicated into a polymeric resist deposited on a substrate. Nanoimprint techniques come in three basic flavors: (i) Thermal imprinting³; (ii) Spin on UV imprinting⁴; and (iii) Liquid dispense based UV imprinting⁵.

[†] Also on the faculty of mechanical engineering at the University of Texas at Austin

[‡] Corresponding author, svsvs@milito.com

Thermal imprinting techniques lead to high pressures and temperatures and are undesirable from the perspective of defectivity, template life and overlay. The UV nano-imprint processes uses UV cross-linking chemicals as imprinting layers. The viscosity of the UV fluid can be tuned low enough so that the fluid filling can be accomplished in the absence of a high compressive pressure, which makes it compatible for low pressure and room temperature processing. Liquid dispense based UV imprinting – known as Step and Flash Imprint Lithography (S-FIL) – is the process primarily discussed in this paper.

Liquid dispensing allows for tailoring of liquid volume dispensed as a function of template feature density variations, and can be used to compensate for evaporation effects. This leads to a robust, versatile process that has been implemented for both the step & repeat and whole wafer printing applications^{6, 7}. As illustrated in Figure 1, the S-FIL process uses low viscosity UV imprint fluids where an array of small drops of the imprint fluids is dispensed in a drop-on-demand manner depending on various process requirements. A more detailed discussion of S-FIL that includes the current status of the template infrastructure, residual layer uniformity, etch, overlay, and throughput is provided in Reference 8.

2 OVERVIEW OF THE DEFECT EXPERIMENTS

The defect experiments were conducted by printing a 13mm by 13mm field on 200mm bare Si wafers. The template included patterns representative of contact holes and metal 1 features. The defect inspection approach used in this study is illustrated in the schematic of Figure 2. The primary template inspection used in this work was KLA 576 DUV mask inspection tools. The incoming wafers (bare Si wafers) were qualified for particles using an SP1 particle detection tool. The primary patterned wafer inspection tool used was KLA 2132. The template inspection allows detection of defects down to less than 100nm as discussed in Section 3. The SP1 particle detection tool also can detect particles down to less than 100nm. The KLA 2132 has a 250nm pixel and can detect patterned defects down to about 150nm where the patterns are created on bare Si wafers. The primary defect program is therefore capable of studying process defects down to about 150nm. This program is complemented by a modest number of high resolution defect detection studies to understand the inspection and process capabilities at resolution of 25nm or less. An NGR 2100 tool was used to study template defects down to 20nm using a process that allowed for direct inspection of chrome-less fused silica templates. A KLA eS32 tool was used to study defects down to 25nm on the imprinted wafers.

Imprint lithography does not have the large amount of historical statistical defect data that is available for photolithography. The primary S-FIL defect program – while only capable of studying defects down to about 150nm – has been very useful for developing a basic understanding of the defect mechanisms that are unique to the S-FIL process. Since this is the first defect study using a fully automated imprint tool, it has led to valuable learning in understanding the potential challenges in obtaining defect data down to the levels required for CMOS manufacturing. The data obtained from this project has helped identify key opportunities for defect reduction, which has led to several orders of magnitude reduction in defect densities as discussed in Section 4. Next, high resolution defect inspection with detection capability of 25nm or less has provided a first look at the nature of defects at leading edge line widths required for sub-32nm CMOS manufacturing.

3 CLASSIFICATION OF S-FIL DEFECTS

Based on the defect data collected using the procedure outlines in Section 2, the defects encountered in the S-FIL process can be classified as shown in Figure 3. There are three primary classes of defects: (i) Template fabrication defects; (ii) S-FIL process defects; and (iii) Defect mechanisms caused by particulate contamination. The nature of these classes of defects and the data obtained that is relevant to each of these defect classes is presented in the next three sub-sections.

3.1 Template Fabrication Defects:

The template fabrication defects include: (i) *High-resolution defects* – These are defects resulting from the e-beam patterning followed by pattern transfer; and (ii) *Ancillary defects*: These are other defects resulting from ancillary

processing that are required to create a template from a photomask blank. The ancillary processes involved in fabricating the templates include a wet etch process step to create a region around the active area that is etched back by about 15 microns; a dice and polish step that creates four templates from each 6025 mask blank; and shipping and automated handling procedures used during fabrication, cleaning, and preparation of the template for use in the S-FIL tool. A detailed discussion of the nature of defectivity observed in these ancillary processes is discussed in more detail in the literature⁹.

The high resolution defects are quantified using KLA DUV mask inspection tools in the mask house. The capability of these tools to inspect template defects was studied using a set of programmed defects and the defects were measured in transmission and reflection modes using a KLA 576. The class of programmed defects that were studied is shown in Figure 4. The smallest programmed defect that can be detected with > 95% capture rate in each class is reported in Figure 5. This data demonstrates that the KLA 576 is sufficient to achieve the goals of the primary defect program as discussed in Section 2 and Figure 2. Also, the NGR 2100 tool has been used to detect defects down to 20nm in direct fused silica e-beam inspections (see example in Figure 6). To-date, these inspections have been used in an isolated manner to understand the limits of e-beam inspection of fused silica; templates inspected in this manner have not been used in wafer defectivity studies.

The ancillary defects tend to include hard template defects referred to here as glass defects, and soft defects which are contaminants acquired by the template during all the ancillary processes. In most cases, the soft defects do not persist through the imprint process due to the self-cleaning nature of the S-FIL process. This feature of the S-FIL process was first reported in the literature several years ago¹⁰, and an example of the same phenomenon is shown in Figure 7.

In the template inspection studies conducted here, the number of high resolution defects detected using KLA 576 were typically less than 5 defects for a template (an active area of 13mm by 13mm). The number of hard defects started out as a high number, but with implementation of processes to manage defects arising from the ancillary processes, these defects are also now below 5 defects per template. The number of soft defects can be as high as 10-100 defects; these are cleaned up by imprint self-cleaning as shown in Figure 7.

3.2 S-FIL Process Defects:

This class of defects includes bubble defects, material left behind on the template due to improper release, and contaminants being dispensed along with the materials as shown in Figure 3. For an optimized material set and process conditions, these defects are typically very low. They do not contribute significantly to overall defectivity. The imprint materials have been purified to eliminate contaminants, including ionic contamination levels to less than 10ppb for obtaining electronic grade materials. These contamination levels are also confirmed for as-dispensed materials to ensure that the dispensers do not add any significant levels of contamination.

A study of S-FIL process defects was performed by using two types of patterned wafer inspection, KLA2132 (250nm pixel inspection) and KLA ES32 (25nm pixel). A comparison of the data is provided for a template that included contact and metal 1 (M1) regions. The template layout is shown in Figure 8. In the defect study, it was found that the contact region had low defectivity, and this region was chosen for studying the S-FIL process defects in this article. On the other hand, the M1 region was found to have a systematic defect mechanism in template fabrication that was not picked up by KLA576 or KLA2132. But it was picked up by KLA ES32. The resulting defect density in the M1 region exceeded 1,000 defects/cm². It has since been established that the defectivity is arising from the high resolution patterning step of template fabrication. Experiments are ongoing to identify the root cause of this defect and to eliminate them in the template fabrication process. Using a review SEM, it was found that the defects seemed to all coming from this high-resolution template fabrication defect. However, the high defect density made it difficult to study any S-FIL specific defect trends. Therefore, the results reported here excluded the M1 region and was confined only to the contact region. The table in Figure 9 shows the total defectivity in a contact region of an imprinted field for both KLA 2132 and KLA eS32. The raw data obtained from the two inspection tools was followed by a review SEM study to eliminate any false defects. The remaining defects were classified into template fabrication defects (repeaters), particle defects, and S-FIL process defects (includes bubbles, release failure, etc.). The data clearly indicates that there are no S-FIL process defects in each case. The increased resolution of the e-beam inspection (KLA eS32) only detects increased particle adders. This result is the first time an imprint lithography process has been studied for defects down to 25nm in a statistically

significant manner. The fact that the S-FIL process defects were observed to be zero in the contact region is very promising. Although this was an experiment with relatively low inspected area, the lack of defect size dependence for both the template defects and the imprint specific defects is very important since it suggests that the density of these defects is not strongly correlated with size. This result is not entirely surprising. Micro-bubbles are known to be less stable the smaller they become, and imprint feature failure due to improper release are known to be more dependent on aspect ratio than feature size. The increase in particles as the resolution of the defect detection improved was to be expected. Further work in a cleaner environment, will reduce these numbers.

3.3 Defects Caused by Particulate Contamination:

As shown in Figure 3, there are three kinds of particle events that affect defectivity in an S-FIL process. Pre-existing front side and back-side wafer particles are the most relevant ones as they disrupt the fluid mechanics associated with the imprint process. The third kind of particle event (post-imprint fall-on particle) is not discussed any further as it has substantially the same impact as any post-processed particle event in semiconductor fabrication.

It is important to note that the template never makes hard contact with the substrate, and the S-FIL process uses low applied forces since it is based on a low viscosity liquid material. There is always a residual film of imprint material between the two surfaces. The thickness of this residual film depends on the type of the etch process utilized for pattern transfer. For a direct tone S-FIL process, the computation of the film thickness for a given half-pitch node is affected by assumptions on the maximum feature aspect ratio (A_r) used and the ratio of the height of the feature to the mean film thickness (H_r) for acceptable etch characteristics. If A_r is assumed to be no greater than 2 and the minimum H_r required is 3, then for the 32nm half-pitch node, then the mean film thickness can be as high as 21nm. For a reverse tone S-FIL process¹¹, assuming that a 3.5:1 aspect ratio can be used during dry etching, the mean film thickness can be as high as 110nm.

The presence of a front-side particle whose height is less than the residual film thickness has no impact on defectivity. If a particle is taller than the thickness of the residual layer, it does cause disruption of the process locally, and a portion of the field being printed is lost. Further, if the particle has a height that is less than the dispensed fluid drops (which typically is 1-2 microns), the imprint fluid drops tend to cushion any impact between the template and the particle. This leads to a low force interaction of the template with the particle. This fact, along with in-situ tool diagnostics, appears to not lead to any template damage as far as the particles are less than the height of the fluid drops. Also, since the template is made from fused silica – a hard and robust material – the template does not get damaged by soft particles. Experience to-date suggests that template damage from front side particle events is rare. It is believed that such damage occurs when the particles are larger than the drop height and the particles are hard inorganic materials. An example of a ~ 10 micron front side particle and the resulting damage from it is shown in Figure 10. The damage is further minimized by use of force sensing in the tool to detect such events and minimize the impact forces resulting from it.

Pre-existing back side particles do not appear to cause template damage. They however do cause disruption of the process locally, and a portion of the field being printed is lost. Pre-existing backside particles also similarly affect photolithography causing “hot spots” that are outside the depth of focus of the optics leading to yield loss in that region. Figure 11 shows random defects in two wafers caused predominantly by back side particle events. In this data, all the repeating defects have been removed.

4 DEFECT DATA TRENDS

The overall trend in total defectivity over the last three years is presented in Figure 12. All of this data was compiled using the KLA 2132 wafer inspection tool. The trend is clearly encouraging considering the semi-log nature of the plot. The plot also indicates key process changes that were implemented to achieve this defect reduction. These process changes include a move to commercial mask houses for template fabrication, improved materials with better understanding of adhesion and release properties, better control over particles in incoming wafers prior to the imprint process, and better understanding of defect mechanisms in the ancillary processes required to create templates out of the 6025 mask blanks fabricated at commercial mask houses.

5 TEMPLATE LIFETIME

As discussed in Section 3.3 templates are surprisingly resistant to damage from front side particle events. This is because the template is robust (fused silica) to soft particles. Particles smaller in height than the residual layer do not touch the template, and particles smaller in height than the dispensed drops (1-2 microns) have a soft impact contact with the template. In-situ diagnostics based on force and image sensors minimize damage due to gross front-side particles.

The other concern that people have relative to imprint templates is regarding template “wear”. Fused silica is not eroded by low viscosity organic liquids or by any typical cleaning and preparation techniques used, provided one avoids techniques that etch fused silica. Repeated use of templates over months followed by cross-section SEMs and CD metrology has demonstrated that the templates do not wear out in the S-FIL process.

6 CONCLUSIONS

The S-FIL process can cost-effectively fabricate sub-50 nm structures with arbitrary pattern complexity. The process has generated significant commercial interest in key market segments such as photonic devices, ultra-high density magnetic media, and displays. The impact of this technology on mainstream silicon fabrication will probably be a direct function of how well a key manufacturing challenge can be overcome: minimizing long-term defects both in the S-FIL process and the template fabrication process to maximize yield. A key future challenge is to develop and demonstrate a process that can approach the long-term yield and productivity of photolithography.

This paper has presented, for the first time, defect results from a fully automated step and repeat imprint process. The defect reduction trends are very encouraging. Also, the data obtained from the KLA eS32 inspection using a 25nm pixel wherein the S-FIL process defects were low indicates that the S-FIL process has the potential to have the defect levels required for CMOS fabrication. Challenges remain including the management of sporadic particle events that disrupt the process, and the need for scale up of the defect study to generate a lot more data to ensure that all the relevant statistical trends are understood. Ongoing research work is seeking to address these topics.

7 ACKNOWLEDGMENTS

The authors would like to thank Mark McCord at KLA Tencor for his assistance in obtaining the eS32 data. The authors would like to acknowledge the team at Molecular Imprints, Inc. for their contributions to this project. This work was partially funded by DARPA Contract No. N66001-02-C-8011, NIST Advanced Technology Program Contract No. 70NANB4H3012, and DoD Contract No. N66001-06-C-2003.

8 REFERENCES

1. International Technology Roadmap for Semiconductors – 2006 Update.
2. F. Hua, Y. Sun, A. Gaur, M. A. Meitl, L. Bilhaut, L. Rotkina, J. Wang, P. Geil, M. Shim, J. A. Rogers, and A. Shim, “Polymer imprint lithography with molecular-scale resolution,” *Nano Lett.* 4(12), 2467–2471 (2004).
3. Chou, S.Y., P.R. Krauss, and P.J. Renstrom, Nanoimprint lithography. *J. Vac. Sci. Tech. B*, 1996. 14(6): p. 4129.
4. M. Otto, M. Bender, F. Richter, B. Hadam, T. Kliem, R. Jede, B. Spangenberg, H. Kurz, “Reproducibility and homogeneity in step and repeat UV-nanoimprint lithography,” *Microelectronic Engineering*, Volume 73-74, Issue 1, June 2004.
5. Colburn, M., et al., Step and Flash Imprint Lithography for sub-100nm Patterning. *Proc. SPIE: Emerging Lithographic Technologies IV*, 2000. 3997: p. 453.
6. D.J. Resnick, S.V. Sreenivasan, C.G. Willson, “Step & flash imprint lithography,” *Mats. Today* 8(2), 34–42, 2005.

7. Doug Resnick, Gerard Schmid, Mike Miller, et al., "High Volume Full-Wafer Step and Flash Imprint Lithography," Solid State Technology, February 2007.
8. C. Mark Melliar-Smith, "Lithography Beyond 32nm – A Role for Imprint?," Plenary Talk, SPIE Advanced Lithography Conference, San Jose, CA, February 26 - March 2, 2007.
9. J. G. Maltabes, J. Brown, J. Perez, "Systematic approach to reducing imprint template defectivity," Paper No. 6349-87, SPIE Photomask Technology 26th Annual Symposium, 18–22 September 2006, Monterey, California USA
10. T. Bailey, B.J. Choi, M. Colburn, A. Grot, M. Meissl, S. Shaya, J.G. Ekerdt, S.V. Sreenivasan, C. G. Willson, "Step and Flash Imprint Lithography: Template Surface Treatment and Defect Analysis", *AVS J. of Vac. Sci. & Tech. B*, Vol. 18, No. 6, Nov/Dec 2000, pp. 3572-3577.
11. S. V. Sreenivasan, I. McMackin, F. Xu, D. Wang, N. Stacey and D. J. Resnick, MICRO Magazine, January 2005.

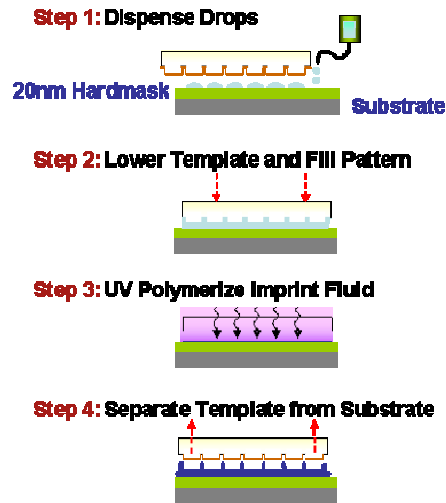


Figure 1: The Step and Flash Imprint Lithography Process

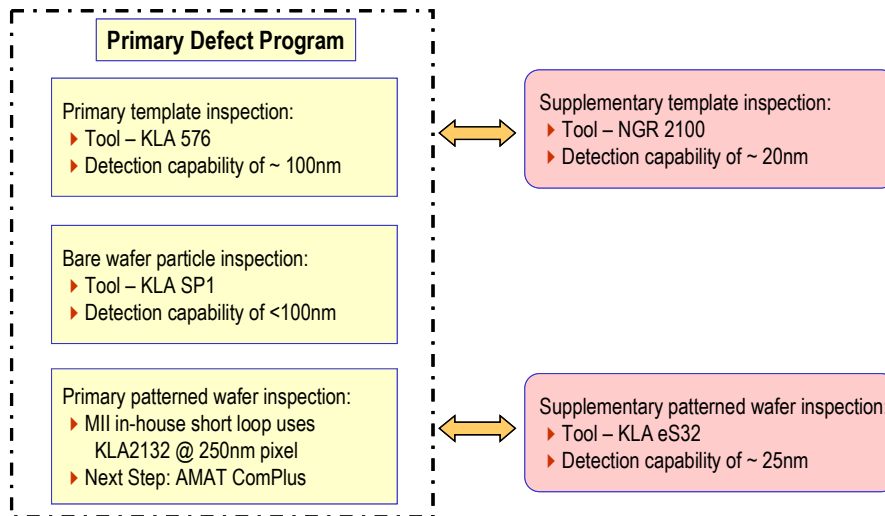


Figure 2: Defect Inspection Approach

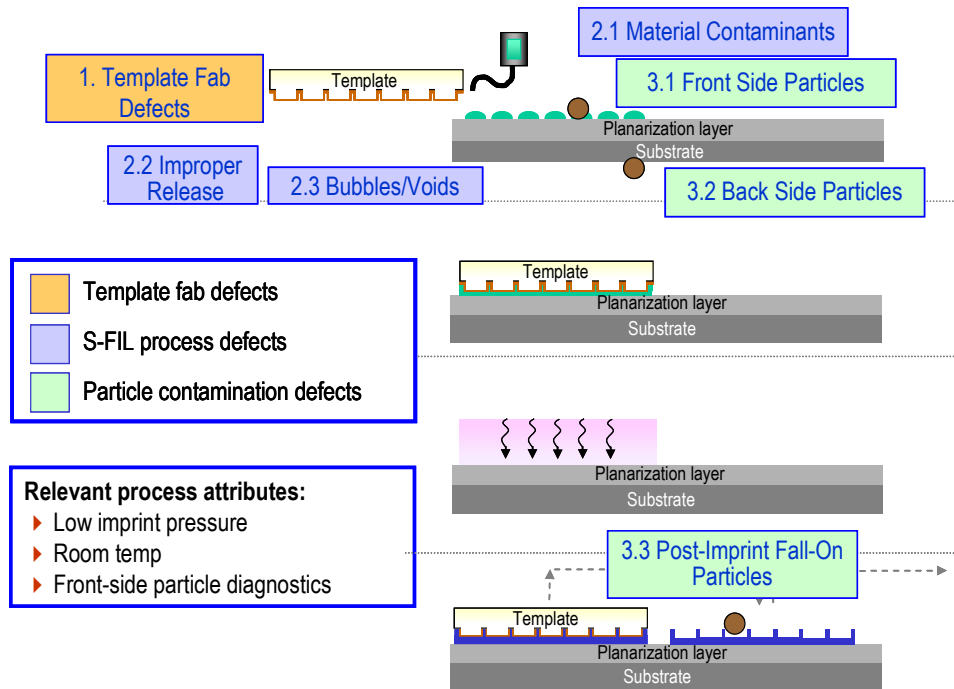


Figure 3: Classification of Defects Encountered in the S-FIL Process

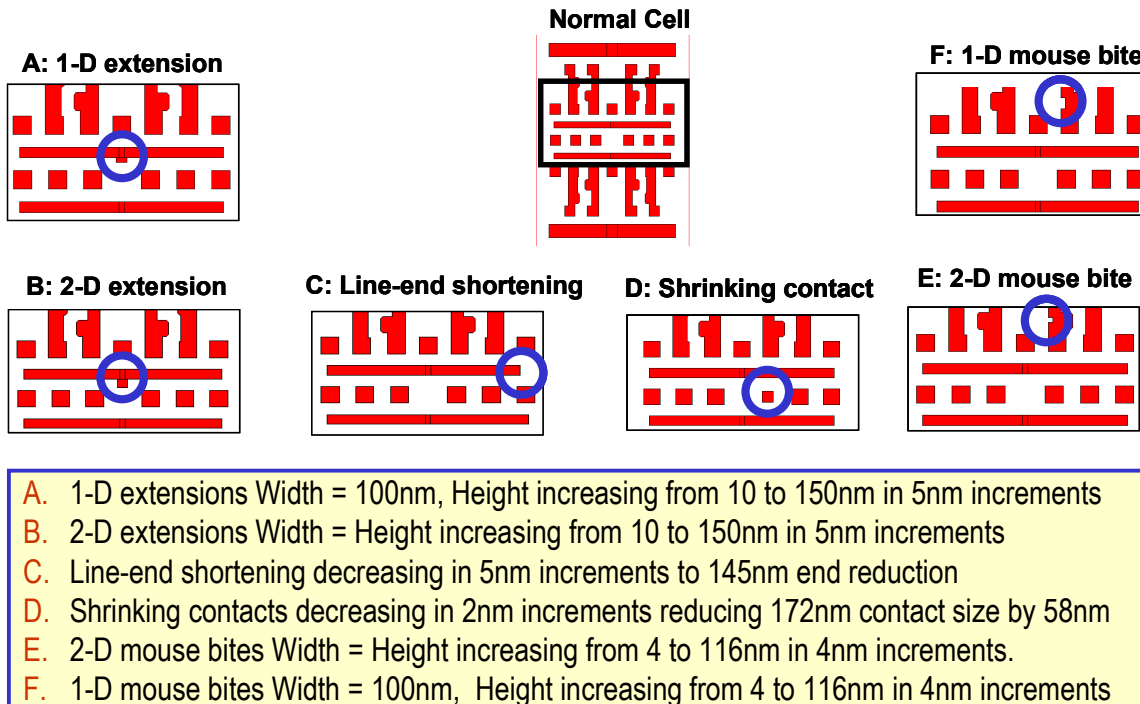


Figure 4: Six classes of programmed defects used for DUV template inspection studies

Defect Type	Binary Cr (nm)	Fused Silica (nm)
Shrinking contact	54	18
1D mouse bite	60	36
2D mouse bite	64	56
1D Extension	65	110
Line End Shortening	75	50
2D extension	95	125

Figure 5: Sensitivity of the six defect classes at 95% capture rate while performing binary Cr and fused silica inspections. Fused silica inspection has better sensitivity in four cases, while the binary inspection has better sensitivity while inspecting 1D and 2D extensions

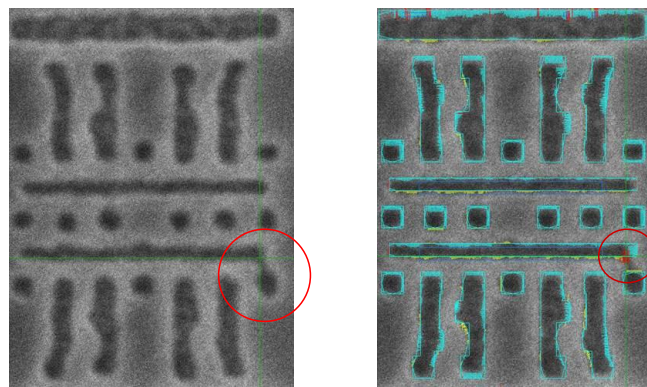


Figure 6: Direct inspection of fused silica in a die-to-database mode shows the detection of a 20nm short defect. This data is courtesy of NGR Corporation in Japan.

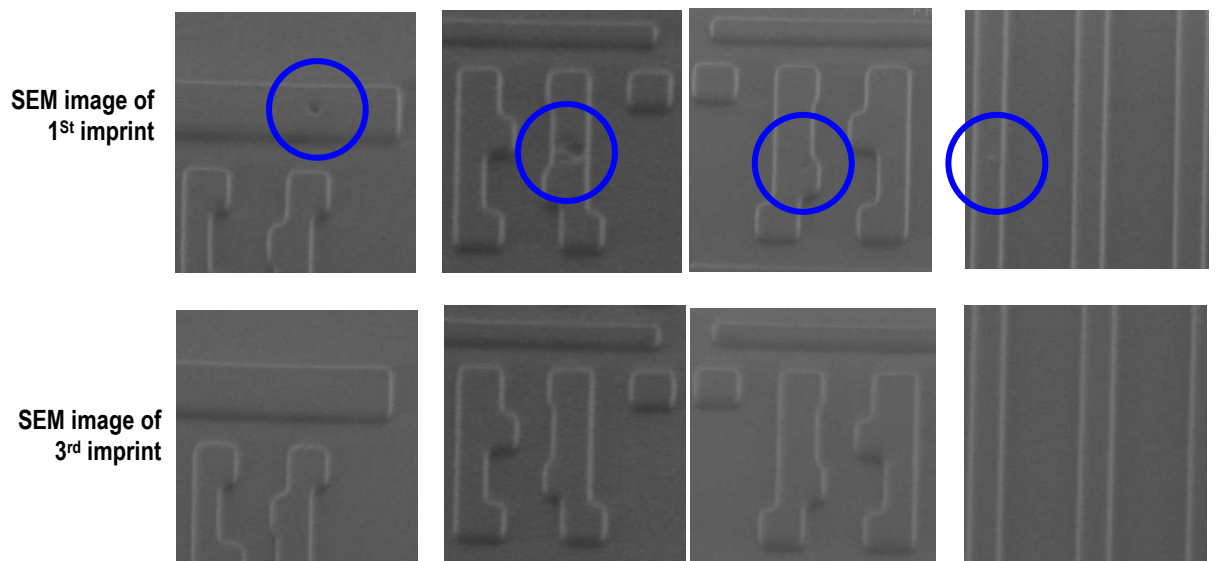


Figure 7: Self-Cleaning of Soft Defects

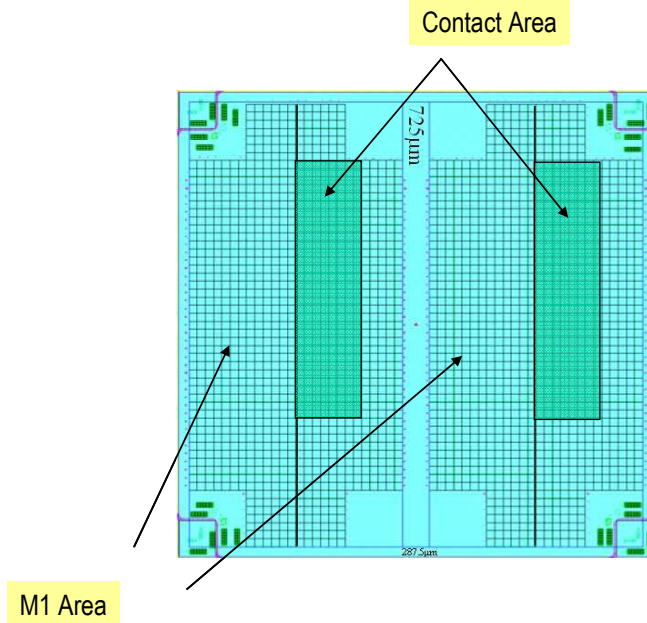


Figure 8: Template with an active area of 13mm by 13mm showing Contact and M1 regions

Defect Class	Defect Count	Defect Density (cm ⁻²)
Template Fabrication	4	4.8
S-FIL Process Related	2	2.4
Particle Related	0	0
Total	6	7.2

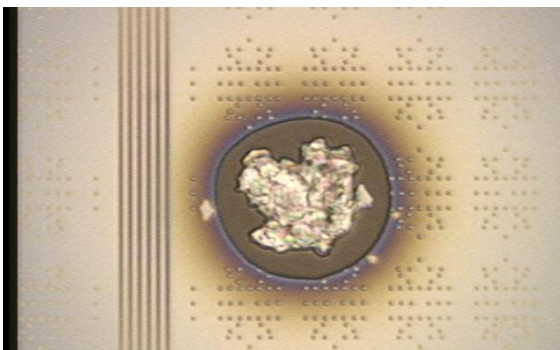
Figure 9 (a): KLA 2132 data

Defect Class	Defect Count	Defect Density (cm ⁻²)
Template Fabrication	4	6
S-FIL Process Related	13	19.7
Particle Related	0	0
Total	17	25.7

Figure 9 (b): Corresponding ES32 data

Figure 9: Defect density data for the contact region of the defect template shown in Figure 8

Front-side particle (>10µm) during imprint



Resulting imprint repeating defect



Figure 10: Front side particle events rarely lead to template damage as described in Section 3.3. An example of a > 10 micron front side particle resulting in a small (~0.25 micron) template defect is shown here.

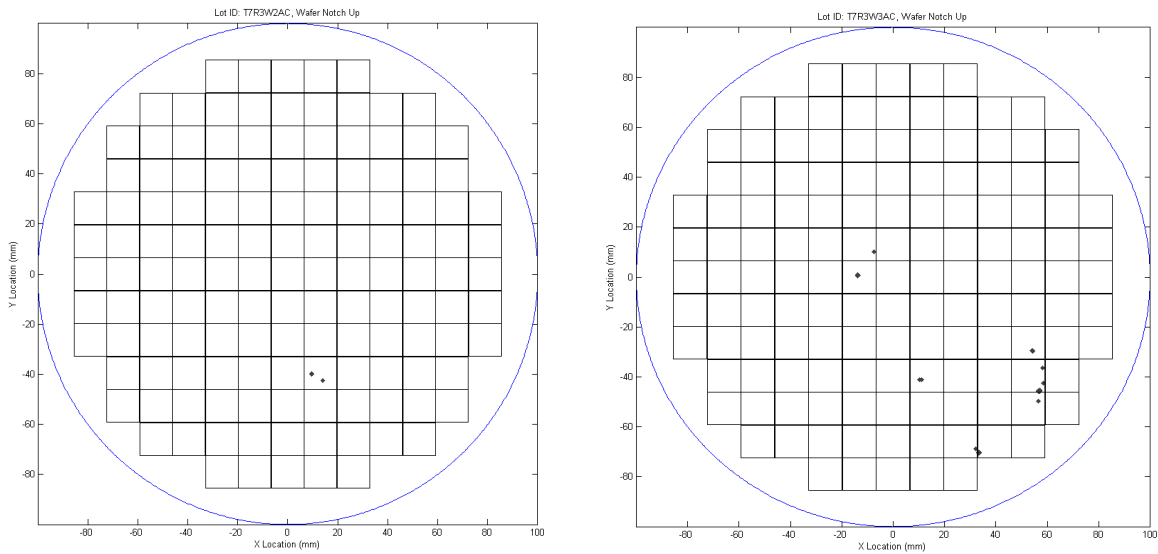


Figure 11: Two wafer maps showing random defects only (repeaters have been removed from this data). The random defects shown here are dominated by back side particle events. This data was obtained using a KLA 2132 with a 250nm pixel detection capability.

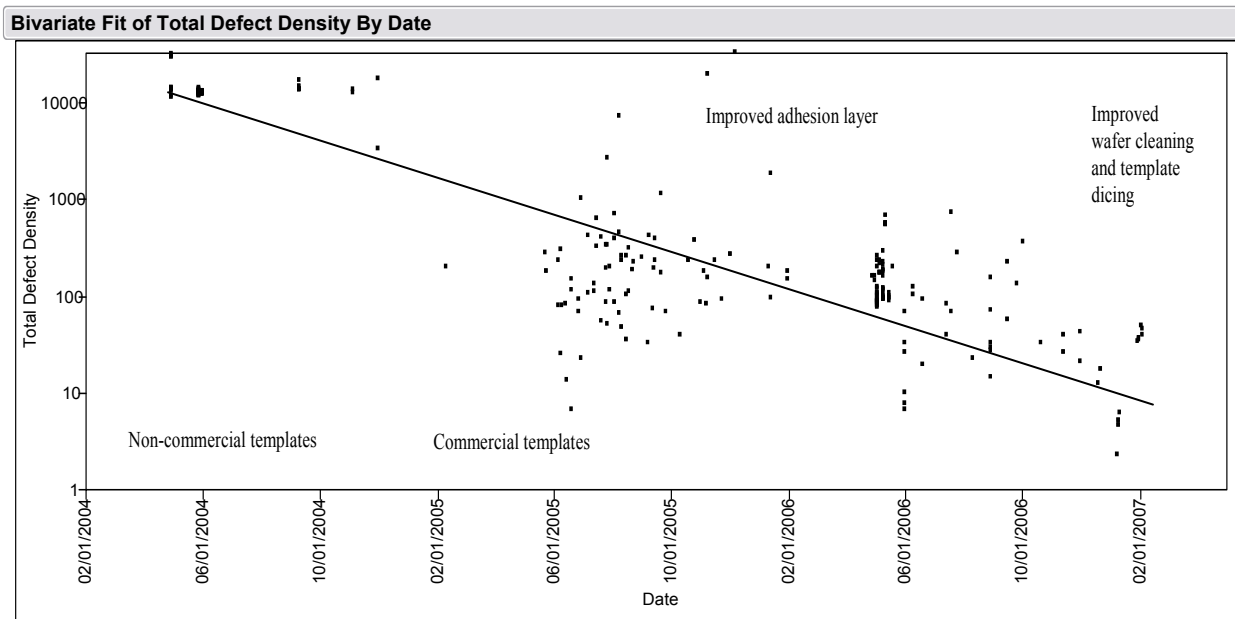


Figure 12: Improvement in total defectivity of the S-FIL process over the last three years.